International Journal of Innovative
Computing, Information and Control
Volume **9**, Number **11**, November **2013**

ICIC International ©2013 ISSN 1349-4198
pp. 4373–4387

AN ENHANCED ENERGY SAVING STRATEGY FOR AN ACTIVE DRX IN LTE WIRELESS NETWORKS

Yan Zhang[1], Shunfu Jin[1] and Wuyi Yue[2]

[1]College of Information Science and Engineering
Yanshan University
No. 438, Hebei Avenue, Qinhuangdao 066004, P. R. China
zy419Lab@163.com; jsf@ysu.edu.cn

[2]Department of Intelligence and Informatics
Konan University
8-9-1, Okamoto, Higashinada-ku, Kobe, Hyogo 658-8501, Japan
yue@konan-u.ac.jp

Received December 2012; revised April 2013

Abstract. *When using a Discontinuous Reception (DRX) mechanism in Long Term Evolution (LTE) for wireless communication of high-speed data, two different operational modes are employed: Idle DRX and Active DRX. In this paper, in order to guarantee a low latency while reducing the energy consumption, we introduce a sleep-delay timer before the system enters into a sleep state from a working state, and consider a strategy to enhance energy saving for the Active DRX where the system switches to a sleep state from a working state. We call the time length of the sleep-delay timer a sleep-delay period and the switching period a waking-up procedure. We build a discrete-time queueing model with two stages of vacations by taking into account the sleep-delay period and the waking-up procedure to model the system operation. By using an embedded Markov chain, we present an exact analysis to numerically evaluate the performance of the system model. We then give the formulas for the performance measures in terms of handover ratio, energy consumption and average latency of the data frames, and present numerical experiments to investigate the influence of the configuration parameters on the system performance. Finally, by considering the trade-off between different performance measures, we optimize the enhanced energy saving strategy for the Active DRX.*

Keywords: DRX, LTE wireless networks, Energy saving strategy, Sleep-delay, Two stages of vacations, Embedded Markov chain

1. **Introduction.** With the development of communication technology, a raft of new applications, such as instant message services, multimedia services and social network services, have imposed higher demands than before for high data transmission rates, greater energy conservation and larger system capacities [1]. The Long Term Evolution (LTE) project for Universal Mobile Telecommunications Systems (UMTs) has been initiated by the Third Generation Partnership Project (3GPP) [2]. The purpose of LTE is to accommodate more users in every cell, accelerate the data transmission rate, and reduce the energy consumption and the cost of the network. Many telecom operators have deployed LTE networks and concentrated their research into LTE productions [3]. Recently, novel techniques in LTE projects have become a focus of research.

As an energy saving strategy, a Discontinuous Reception (DRX) mechanism is defined in the medium access control (MAC) specification of LTE [4]. There are two operational modes in the DRX mechanism, i.e., Idle DRX and Active DRX [5]. For an Idle DRX, the system stays in the Radio Resource Control IDLE (RRC_IDLE) state when there is

no data frame in the user's buffer. If a data frame arrives, the User Equipment (UE) will send an RRC request and rebuild the port connection to an evolved NodeB (eNB). For an Active DRX, the system stays in the state of RRC_CONNECTED even if there is no data frame to be transmitted or to be received. However, the UE will shut down the transmitter-receiver unit temporarily to save energy. When there is a data frame to be transmitted or received, the UE will switch into the working state from the sleep state directly without rebuilding the RRC connection with an eNB and the signaling overhead will be decreased [6].

Recently, many energy saving strategies in DRXs have been investigated. For example, Bontu and Illidgee explained the energy saving methods for both a network attached mode and a network idle mode in LTE [7]. They then defined the optimum criteria for different applications in the RRC_CONNECTED and RRC_IDLE states. They found that through the reasonable setting of the DRX parameters, energy could be saved. Yin proposed a simple but efficient application aware DRX mechanism to optimize the system performance of LTE-Advanced networks with Carrier Aggregation (CA) [8]. With CA technology, the UE could support high transmission rates over a wider bandwidth, and the enhanced DRX was able to achieve nearly 50% energy saving compared with the conventional DRX mechanism. Li et al. provided a novel algorithm in which the cycle length of the DRX was adjusted dynamically to realize the variable growth of the sleep cycle [9]. The result of simulation experiments in [9] indicated that the algorithm had an improved effect on the energy saving.

Conclusively, most available research into DRX mechanisms has been focused on improving energy savings to the system or optimizing the system parameters. Moreover, performance evaluations of the DRX mechanism have relied solely on simulation experiments. In pursuing greater energy conservation in the DRX mechanism, a lesser latency is another important constraint on the QoS of wireless networks. However, in order to improve the system performance of the DRX mechanism, very accurate models that faithfully reproduce the stochastic behavior must be produced.

In this paper, we propose an enhanced energy saving strategy for the Active DRX by introducing a sleep-delay timer before the system enters into a sleep state from a working state and we consider a procedure where the system switches to a sleep state from a working state. For this, we build a discrete-time queueing model with two stages of vacations, taking into account the sleep-delay period and the waking-up procedure in order to model the system operation. Moreover, we exactly analyze the system model by using a discrete-time Markov chain and numerically evaluate the performance measures with regard to handover ratio, energy consumption and average latency of the data frames. Finally, we optimize the enhanced energy saving strategy by considering a trade-off between different performance measures. The numerical experiments and system optimizations show that the overall performance of the enhanced energy saving strategy proposed in this paper is superior to that of the conventional Active DRX in LTE.

The structure of this paper is organized as follows. In Section 2, we present an enhanced energy saving strategy of an Active DRX and build a discrete-time multiple-vacation queueing model with vacation delay period and set-up period to model the system operation. In Section 3, we analyze the system model in the steady state. In Section 4, we calculate the formulas for the performance measures. In Section 5, numerical experiments are provided, and the enhanced energy saving strategy for the Active DRX is optimized. Conclusions for this paper are drawn in Section 6.

2. **An Enhanced Energy Saving Strategy and System Model.**

In an Active DRX mechanism of LTE, the DRX cycle is divided into a short DRX stage and a long DRX

stage. The threshold K is set to restrict the number of the short DRX stages in a DRX cycle. Obviously, a larger number of the short DRX stages in a DRX cycle will shorten the average latency of the data frames. On the other hand, a lesser value of K corresponds to a higher number of long DRX stages in a DRX cycle, which will be beneficial for terminal energy conservation [10]. Therefore, a reasonable threshold K will make the system more effective.

In order to guarantee a low latency while reducing the energy consumption, we introduce a sleep-delay timer before the system enters into a sleep state from a working state, and we adopt a procedure where the system switches to a sleep state from a working state, resulting in an enhanced energy saving strategy in the DRX. The time period within the time length of the sleep-delay timer is called a sleep-delay period and the maximal length of the sleep-delay period is denoted as T. During the procedure where the system switches to a sleep state from a working state, the transmitter-receiver unit should be activated. We call this procedure a waking-up procedure.

The working principle of the enhanced energy saving strategy for the DRX in LTE is given as follows:

(1) When all the data frames in the buffer are completely transmitted, a sleep-delay timer will be activated and the system will enter into the sleep-delay period from the working state. If there is a data frame arrival within the sleep-delay period, the sleep-delay period will end at once and the data frame will be transmitted immediately. However, if there is no data frame arrival within the sleep-delay period, the system will switch into a short DRX stage after the sleep-delay timer expires.

(2) If there is at least one data frame arrival in a short DRX stage, the system will initiate a waking-up procedure and then enter into the working state. If there are no data frames arriving during a short DRX stage, and the number of short DRX stages is less than the threshold K, the system will continue with another short DRX stage when the previous short DRX stage is over. If the number of short DRX stages reaches the threshold K and there has still been no data frame arrival, a long DRX stage will begin after the last short DRX stage is finished.

(3) If a data frame arrives during a long DRX stage, when the long DRX stage is over, the system will initiate a waking-up procedure and then enter into a working state. Otherwise, the system will start a new long DRX stage until there is a data frame arrival.

This process will be repeated.

The working principle of the enhanced energy saving strategy of an Active DRX with a slotted structure in LTE is illustrated in Figure 1.

In the enhanced energy saving strategy of an Active DRX mechanism, a shorter time length for the sleep-delay timer will make the system enter into the sleep state quickly. This will reduce the average latency of data frames, but will increase the energy consumption. However, a shorter time length will also cause the system to switch between

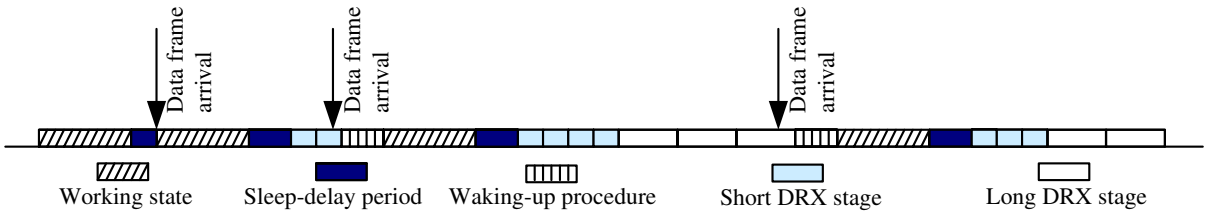

FIGURE 1. Working principle of the enhanced energy saving strategy of an active DRX in LTE

the sleep state and the working state frequently, and the system handover ratio will increase. On the other hand, for a larger threshold for the short DRX stages, the system will spend more time in the short DRX stages. This will decrease the energy conservation and increase the system handover. A larger threshold for the short DRX stages has the advantage of reducing the average latency of data frames. Therefore, the values of the time length of the sleep-delay timer and threshold for the short DRX stages play an important role in the application of the Active DRX in LTE.

Obviously, to evaluate the system performance mathematically, the system model should be constructed reasonably and the values for the system parameters should be set optimally.

The sleep-delay period is seen as a vacation delay period D, and the time length of D is denoted as T_D. The short DRX stage and the long DRX stage are regarded as the short vacation period V_1 and the long vacation period V_2, respectively. The time lengths of the short vacation period V_1 and the long vacation period V_2 are denoted as T_{V_1} and T_{V_2}, respectively. The time period from the instant that the first short vacation period V_1 begins to the instant that the waking-up procedure begins is regarded as a system vacation V. One or more short vacation periods V_1 and long vacation periods V_2 combine to constitute a system vacation V, and the time length of V is denoted as T_V.

We regard the waking-up procedure as a set-up period U. Let T_U denote the time length of U. The time period for the data frames being transmitted continuously is seen as a busy period B, and its length is denoted as T_B. A busy cycle R is defined as the time period from the instant that a busy period B ends to the instant that the next busy period B ends. The busy cycle can be regarded as the DRX cycle in LTE.

A queueing model with two stages of vacations is built considering the vacation delay period and the set-up period in this paper. The state transition of this queueing model is illustrated in Figure 2, where K is the maximum number of short vacation periods V_1 in a busy cycle.

3. **Performance Analysis.**

To comply with the digital nature of modern communication, we evaluate the system performance by using a discrete-time queueing model.

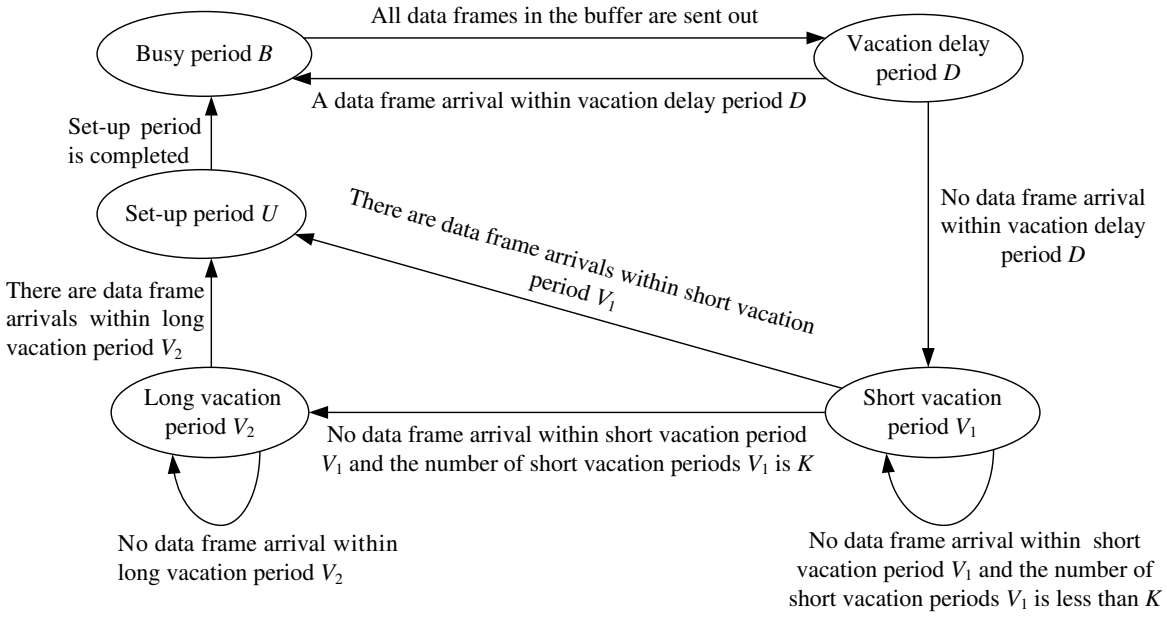

FIGURE 2. The state transition of the queueing model presented in this paper

In this discrete-time queueing model, the time axis is segmented into a series of equal intervals called slots. The data frame arrivals or departures are supposed to happen only at the boundary of a slot. A single channel and an infinite capacity are considered in this model. The transmissions of data frames are supposed to follow a First-Come First-Served (FCFS) discipline.

Moreover, for the sake of analytical tractability, we assume that the arrival process of data frames follows a Bernoulli distribution, such that a data frame arrives in a slot with probability p $(0 < p < 1)$, and no data frame arrives in a slot with probability q, $q = 1-p$. The transmission time S of a data frame is supposed to follow a general distribution. Let the transmission time S of a data frame be an independent and identically distributed random variable. The probability distribution s_k, the Probability Generating Function (PGF) $S(z)$ and the average value $E[S]$ of S can be expressed as follows:

$$P\{S = k\} = s_k, \quad k = 1, 2, \ldots, \quad S(z) = \sum_{k=1}^{\infty} s_k z^k, \quad E[S] = \sum_{k=1}^{\infty} k s_k.$$

We select the departure instant of every data frame as the embedded Markov point and define the state of the system by the number of data frames at these embedded Markov points. So the system structure at the embedded points constitutes an embedded Markov chain. The sufficient and necessary condition for the embedded Markov chain to be steady is $\rho = pE[S] < 1$.

3.1. **Busy period analysis.** In this system model, a busy period B begins either at the completion moment of a vacation delay period D because there is a data frame arrival, or at the instant that a set-up period U ends. The set-up period U begins with a short vacation period V_1 or a long vacation period V_2, during which there is at least one data frame arrival.

Let P_D be the probability that there is a data frame arrival in the vacation delay period D. For this case, the system will enter into a busy period B directly from the vacation delay period D. P_D can be given as follows:

$$P_D = 1 - q^T. \tag{1}$$

Let P_{V_1} be the probability that the system will switch into the set-up period U from a short vacation period V_1, and P_{V_2} be the probability that the system will enter into the set-up period U from a long vacation period V_2. P_{V_1} and P_{V_2} can be given as follows:

$$P_{V_1} = 1 - q^{KT_{V_1}}, \quad P_{V_2} = q^{KT_{V_1}}. \tag{2}$$

Let $A_j^{V_1}$ be the probability that there are j data frame arrivals during a short vacation period V_1 given that there is at least one data frame arrival in this short vacation period. $A_j^{V_1}$ is given as follows:

$$A_j^{V_1} = \frac{p^j q^{T_{V_1}-j}}{1 - q^{T_{V_1}}}, \quad j \geq 1. \tag{3}$$

Let $A_j^{V_2}$ be the probability that there are j data frame arrivals during a long vacation period V_2 given that there is at least one data frame arrival in this long vacation period. $A_j^{V_2}$ is given as follows:

$$A_j^{V_2} = \frac{p^j q^{T_{V_2}-j}}{1 - q^{T_{V_2}}}, \quad j \geq 1. \tag{4}$$

Let A_V be the number of data frames that have arrived at the beginning instant of a set-up period U. The probability distribution of A_V can be given as follows:

$$P\{A_V = j\} = \begin{cases} P_{V_1} A_j^{V_1} + P_{V_2} A_j^{V_2}, & 1 \le j \le T_{V_1} \\ P_{V_2} A_j^{V_2}, & T_{V_1} + 1 \le j \le T_{V_2}. \end{cases} \tag{5}$$

Accordingly, the PGF $A_V(z)$ of A_V can be given as follows:

$$\begin{aligned} A_V(z) &= \sum_{j=1}^{T_{V_1}} P\{A_V = j\} z^j + \sum_{j=T_{V_1}+1}^{T_{V_2}} P\{A_V = j\} z^j \\ &= P_{V_1} \times \frac{(q+pz)^{T_{V_1}} - q^{T_{V_1}}}{1 - q^{T_{V_1}}} + P_{V_2} \times \frac{(q+pz)^{T_{V_2}} - q^{T_{V_2}}}{1 - q^{T_{V_2}}}. \end{aligned} \tag{6}$$

Differentiating Equation (6) with respect to z at $z = 1$, the average value $E[A_V]$ of A_V can be obtained as follows:

$$E[A_V] = P_{V_1} \times \frac{pT_{V_1}}{1 - q^{T_{V_1}}} + P_{V_2} \times \frac{pT_{V_1}}{1 - q^{T_{V_2}}}. \tag{7}$$

Supposing the time length T_U of a set-up period follows a general distribution, the probability distribution u_k, PGF $T_U(z)$ and average value $E[T_U]$ of T_U will be obtained as follows:

$$u_k = P\{T_U = k\}, \quad k = 1, 2, \ldots, \quad T_U(z) = \sum_{k=1}^{\infty} u_k z^k, \quad E[T_U] = \sum_{k=1}^{\infty} k u_k. \tag{8}$$

By letting A_U be the number of data frames that have arrived during a set-up period U, the PGF $A_U(z)$ can be obtained as follows:

$$A_U(z) = \sum_{j=0}^{k} \sum_{k=1}^{\infty} u_k \binom{k}{j} p^j q^{k-j} z^j = T_U(q + pz). \tag{9}$$

Differentiating Equation (9) with respect to z at $z = 1$, the average value $E[A_U]$ of A_U is given as follows:

$$E[A_U] = pE[T_U]. \tag{10}$$

A busy period B begins given one of the following two cases:

(1) If there is a data frame arrival within the maximum length T of a vacation delay period D, the arriving data frame will trigger a busy period B immediately. The probability of this event is P_D, which is given in Equation (1). Letting Q_{B_1} be the number of data frames at the beginning instant of a busy period B in this case, the PGF $Q_{B_1}(z)$ of the Q_{B_1} is given as follows:

$$Q_{B_1}(z) = z. \tag{11}$$

(2) If there is no data frame arrival in the vacation delay period D, the system vacation period V will begin when a vacation delay period D is over. The probability that there is no data frame arrival during the vacation delay period D is q^T. When the vacation period is over, the system will firstly go through a set-up period U, and then enter into a busy period. For this case, letting Q_{B_2} be the number of data frames at the beginning instant of a busy period B, the PGF $Q_{B_2}(z)$ of Q_{B_2} can be obtained as follows:

$$Q_{B_2}(z) = A_V(z) A_U(z). \tag{12}$$

Let Q_B be the number of data frames at the beginning instant of a busy period B. Taking into account both cases mentioned above, we can obtain the PGF $Q_B(z)$ of Q_B as follows:

$$Q_B(z) = (1-q^T)Q_{B_1}(z) + q^T Q_{B_2}(z). \tag{13}$$

Differentiating Equation (13) with respect to z at $z=1$, the average value $E[Q_B]$ of Q_B can be given by

$$\begin{aligned} E[Q_B] &= 1 - q^T + q^T E[A_V] + q^T E[A_U] \\ &= pH \end{aligned} \tag{14}$$

where H is given as follows:

$$H = \frac{1-q^T}{p} + \frac{q^T P_{V_1} T_{V_1}}{1-q^{T_{V_1}}} + \frac{q^T P_{V_2} T_{V_2}}{1-q^{T_{V_2}}} + q^T E[T_U]. \tag{15}$$

3.2. **Queueing length and waiting time.** At the embedded point, the steady state queueing length L^+ can be decomposed into two parts, i.e., $L^+ = L_0 + L_d$. L_0 is the queueing length of the classical Gemo/G/1 model, and L_d is the additional queueing length introduced by the multiple vacations.

The average value $E[L_0]$ of L_0 can be given as follows:

$$E[L_0] = \frac{p^2 E[S(S-1)]}{2(1-\rho)}. \tag{16}$$

By using the boundary state variable theory [11], the PGF of L_d is given as follows:

$$L_d(z) = \frac{1-Q_B(z)}{E[Q_B](1-z)}. \tag{17}$$

Differentiating Equation (17) with respect to z at $z=1$, the average value $E[L_d]$ of L_d is obtained as follows:

$$\begin{aligned} E[L_d] &= \frac{E[Q_B(Q_B-1)]}{2E[Q_B]} \\ &= \frac{pq^T}{2H} \times \left(P_{V_1} T_{V_1} \frac{(T_{V_1}-1) + 2E[T_U]}{1-q^{T_{V_1}}} + P_{V_2} T_{V_2} \frac{(T_{V_2}-1) + 2E[T_U]}{1-q^{T_{V_2}}} \right). \end{aligned} \tag{18}$$

Combining Equations (16) and (18), the average value $E[L^+]$ of L^+ can be given as follows:

$$E[L^+] = E[L_0] + E[L_d]. \tag{19}$$

Using Little's law [11], the average waiting time $E[W]$ of data frames is obtained as follows:

$$E[W] = \frac{E[L^+]}{p} = \frac{q^T}{2H} \times \left(P_{V_1} T_{V_1} \frac{(T_{V_1}-1) + 2E[T_U]}{1-q^{T_{V_1}}} + P_{V_2} T_{V_2} \frac{(T_{V_2}-1) + 2E[T_U]}{1-q^{T_{V_2}}} \right). \tag{20}$$

3.3. **Busy cycle analysis.** Note that a busy cycle is regarded as the DRX cycle in LTE. If there is a data frame arrival within the vacation delay period D, the busy cycle R will consist of a vacation delay period D and a busy period B. Otherwise, a busy cycle R will include a vacation delay period D, a system vacation period V, a set-up period U and a busy period B.

Note that T is the maximum length of a vacation delay period D, and T_D is the actual length of D, so we have $T_D \le T$. The probability distribution and the average value $E[T_D]$ of the actual length T_D are given as follows:

$$P\{T_D = j\} = \begin{cases} q^{j-1}p, & 0 < j < T \\ q^{T-1}, & j = T, \end{cases} \tag{21}$$

$$E[T_D] = \sum_{j=1}^{T} jP\{T_D = j\} = \frac{1-q^T}{p}. \tag{22}$$

By applying the boundary state variable theory [11], the average value $E[T_B]$ of the busy period B is given as follows:

$$E[T_B] = E[Q_B]\frac{E[S]}{1-\rho} = \frac{\rho H}{1-\rho}. \tag{23}$$

Let N_V be the number of vacation periods in a busy cycle, including the short vacation periods V_1 and long vacation periods V_2. The probability distribution of N_V can be obtained as follows:

$$P\{N_V = j\} = \begin{cases} (q^{T_{V_1}})^{j-1}(1-q^{T_{V_1}}), & 1 \le j \le K \\ (q^{T_{V_1}})^{K}(q^{T_{V_2}})^{j-K-1}(1-q^{T_{V_2}}), & j > K. \end{cases} \tag{24}$$

The average length $E[T_V]$ of the system vacation V is then given as follows:

$$\begin{aligned} E[T_V] &= \sum_{j=1}^{K} jT_{V_1}P\{N_V = j\} + \sum_{j=K+1}^{\infty}(KT_{V_1} + (j-K)T_{V_2})P\{N_V = j\} \\ &= \frac{P_{V_1}T_{V_1}}{1-q^{T_{V_1}}} + \frac{P_{V_2}T_{V_2}}{1-q^{T_{V_2}}} \end{aligned} \tag{25}$$

where P_{V_1} and P_{V_2} are given in Equation (2).

Let T_R be the time length of a busy cycle period R, and $E[T_R]$ be the average value of T_R. Combining Equations (8), (15), (22), (23) and (25), $E[T_R]$ can be calculated as follows:

$$E[T_R] = E[T_D] + E[T_B] + q^T E[T_V] + q^T E[T_U] = \frac{H}{1-\rho}. \tag{26}$$

4. **Performance Measures.** Let β be the system handover ratio which accounts for the number of switches between the working state and the sleep state per slot. The system handover will occur only when there are no data frame arrivals within the time length of the sleep-delay timer in a DRX cycle. So the handover ratio β can be obtained as follows:

$$\beta = \frac{q^T}{E[T_R]}. \tag{27}$$

The energy saving ratio γ is defined as the energy conservation per slot due to introduction of the sleep mode. Energy is consumed normally in the working state, and is saved in the DRX stages. The system also loses some energy when the system switches between the working state and the sleep state. We express the energy saving ratio γ using the following equation:

$$\gamma = \frac{(C_A - C_S)E[T_V]}{E[T_R]} - \beta C_W \tag{28}$$

where C_A and C_S are the energy consumption per slot in the working state and the DRX stage, respectively, C_W is the energy consumption for each switch from the sleep state to the working state.

We define the latency of a data frame as the time period from the arrival moment of a data frame to the end moment of the transmission of that data frame. Obviously, the average latency σ is the sum of the average waiting time W and the average transmission time S of data frames. Therefore, σ can be given as follows:

$$\sigma = E[W] + E[S]. \tag{29}$$

5. **Numerical Experiments and System Optimizations.** In this section, using numerical experiments and cost functions, the performance of the enhanced energy saving strategy of DRX in LTE is investigated and optimized.

5.1. **Numerical experiments.** In practice, the system parameters, such as the time length for one slot, the arrive rate of data frames, the average transmission time of a data frame, the time length of the waking-up procedure, the energy consumption per second during the working state and the sleep state, and the energy consumption for each switch from the sleep state to the working state, are set as needed.

In this paper, we take 1 slot = 1 ms, $p = 0.05$, $E[S] = 4$ ms, $E[T_U] = 1$ ms, $C_A = 80$ mW, $C_S = 5$ mW, $C_W = 5 \times 10^{-3}$ J as examples by referencing [12].

Figure 3 examines how the handover ratio β changes in relation to the threshold K of the short stages with different time lengths T of the sleep-delay timer, T_{V_1} of the short DRX stage, and T_{V_2} of the long DRX stage.

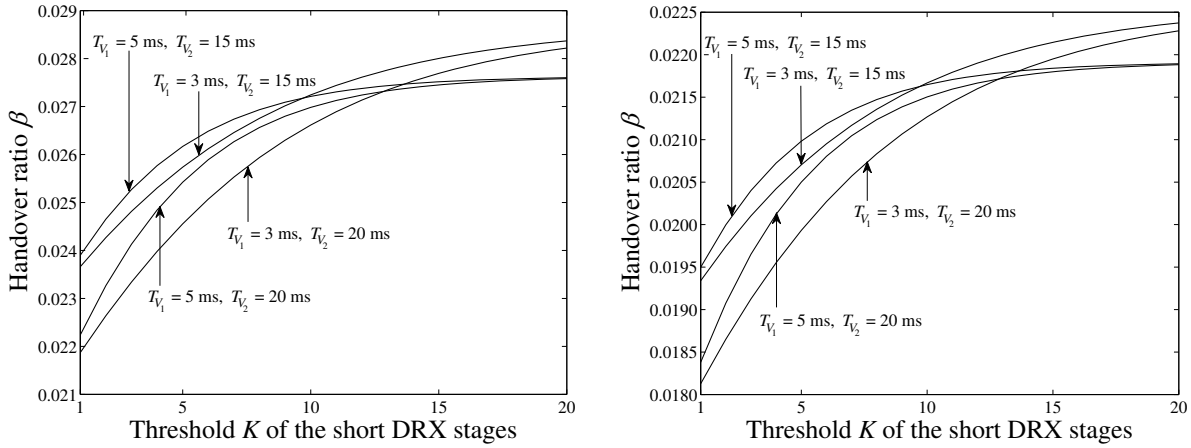

(a) $T = 5$ ms (b) $T = 10$ ms

FIGURE 3. Change trend of the handover ratio

In both Figures 3(a) and 3(b), we find that for all the time lengths T_{V_1} of the short DRX stage and T_{V_2} of the long DRX stage, when the threshold K increases, the handover ratio β will also increase. The reason is that as the threshold K increases, the number of the short DRX stages in a DRX cycle will increase. This increases the likelihood that there will be more data frame arrivals in the short DRX stage, so the system will switch into the working state from the sleep state earlier, meaning the handover ratio will inevitably increase.

In Figures 3(a) and 3(b), we see that for the same time length T_{V_2} of the long DRX stages, when the threshold K is small, the shorter the time length T_{V_1} of the short DRX stage is, and the smaller the handover ratio β will be. For example, for the case $T_{V_2} = 15$ ms and $K < 10$ in Figure 3(a), the handover ratio β with $T_{V_1} = 5$ ms is greater than the handover ratio β with $T_{V_1} = 3$ ms. Note that a smaller threshold K means a lesser number of short DRX stages in a DRX cycle. In this case, if the time length of the short DRX stage is also short, the system will more likely enter into a long DRX stage from the short DRX stage. Because the system will not easily enter into the working state from the long DRX stages, the handover ratio will be lower.

However, when the threshold K is high enough, for example when $K \geq 10$, the shorter the time length T_{V_1} of the short DRX stage is, the greater the handover ratio β will be. In this case, when the threshold K is higher, the number of short DRX stages in a DRX cycle will also be higher, and the data frames will more likely arrive in the short DRX

stages. If the time length of the short DRX stage is shorter, the system will enter into the working state from the short DRX stage more quickly, so the handover ratio will be higher.

Additionally, Figures 3(a) and 3(b) show that for all the time lengths T of the sleep-delay timer, if the threshold K and T_{V_1} of the short DRX stage are the same, a longer time length T_{V_2} of the long DRX stage has a beneficial effect on the handover ratio β. This is because the system cannot switch quickly to the working state from a long DRX stage with a long time length, so the handover ratio will be lower.

Moreover, by comparing Figure 3(a) with Figure 3(b), it is illustrated that for the same threshold K, the same time lengths T_{V_1} of the short DRX stages and T_{V_2} of the long DRX stages, the handover ratio β with a shorter time length T for the sleep-delay timer will be higher than that with a longer time length T. The reason is that a shorter time length for the sleep-delay timer will force the system to enter the sleep state more easily, leading to a higher handover ratio.

Figure 4 demonstrates how the energy saving ratio γ changes as a function of the threshold K for the short stages with different time lengths T for the sleep-delay timer; T_{V_1} for the short DRX stage and T_{V_2} for the long DRX stage.

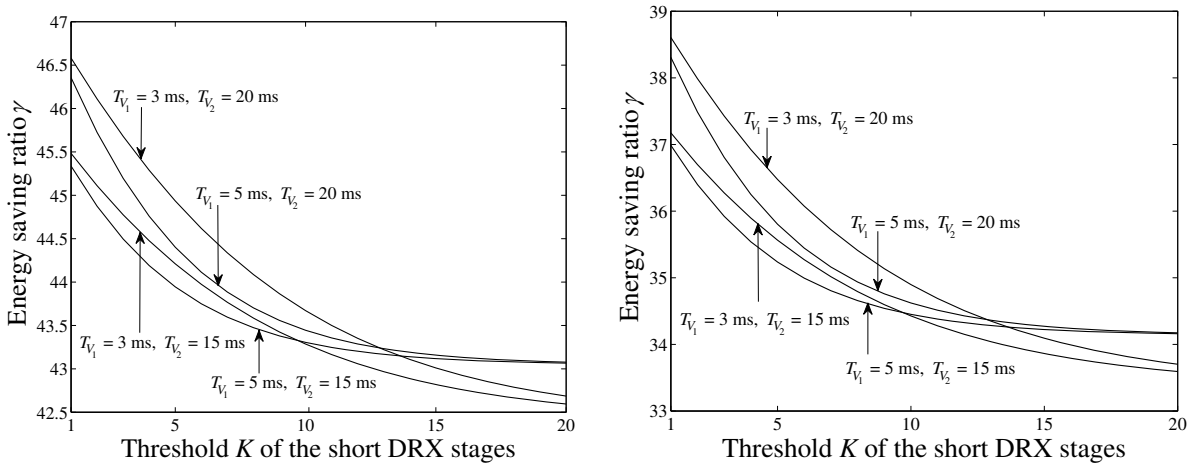

(a) $T = 5$ ms (b) $T = 10$ ms

FIGURE 4. Change trend of the energy saving ratio

In Figures 4(a) and 4(b), we notice that for all the time lengths T_{V_1} of the short DRX stage and T_{V_2} of the long DRX stage, when the threshold K increases, the energy saving ratio γ will decrease. Note that a larger threshold K means there will be more short DRX stages before the system enters into a sleep state. The energy conservation mainly focuses on the DRX stages. The short DRX stages conserve less energy than the long DRX stages for energy conservation. Therefore, less energy will be saved when there is a greater number of short DRX stages, and the energy saving ratio will decrease.

In Figures 4(a) and 4(b), we also observe that for the same time length T_{V_2} of the long DRX stages, when the threshold K is small, the shorter the time length T_{V_1} of the short DRX stage is, and the higher the energy saving ratio γ will be. For example, in the case where $T_{V_2} = 15$ ms and $K < 10$ in Figure 4(a), the energy saving ratio γ with $T_{V_1} = 3$ ms is higher than the energy saving ratio γ with $T_{V_1} = 5$ ms. Note that a smaller threshold K means a lesser number of short DRX stages in a DRX cycle. In this case, if the time length of the short DRX stage is shorter, the system will more likely enter into the long DRX stage from the short DRX stage. As more energy will be saved in the long DRX stages, this will result in an energy saving ratio.

However, when the threshold K is high enough, for example $K \geq 10$, the shorter the time length T_{V_1} of the short DRX stage is, the lower the energy saving ratio γ will be. The reason is that when the threshold K is higher, the number of short DRX stages in a DRX cycle will be greater, so the more likely it will be that there will be a data frame arrival during the short DRX stages. In this case, the smaller the time length T_{V_1} of the short DRX stage is, the more quickly the system will switch to the working state, the less energy will be saved, and the energy saving ratio will be lower.

Additionally, Figures 4(a) and 4(b) illustrate that for the same threshold K and same time length T_{V_1} of the short DRX stages, a longer time length T_{V_2} will result in a higher energy saving ratio γ. This is because the long DRX stages are beneficial to energy conservation, so the energy saving ratio will be higher.

Moreover, by comparing Figure 4(a) with Figure 4(b), it is illustrated that for all the same thresholds K, the same time lengths T_{V_1} of the short DRX stage and T_{V_2} of the long DRX stage, the energy saving ratio γ where time length T of the sleep-delay timer is short, will be greater than that one with a long T. The reason is that a shorter time length of the sleep-delay timer will force the system to enter the DRX stage more easily. Note that energy is saved in DRX stages. Obviously, a shorter sleep-delay timer length will result in a higher energy saving ratio.

Figure 5 illustrates the change trend for the average latency of data frames σ versus the threshold K for the short stages with different time lengths T of the sleep-delay timer, T_{V_1} of the short DRX stage and T_{V_2} of the long DRX stage.

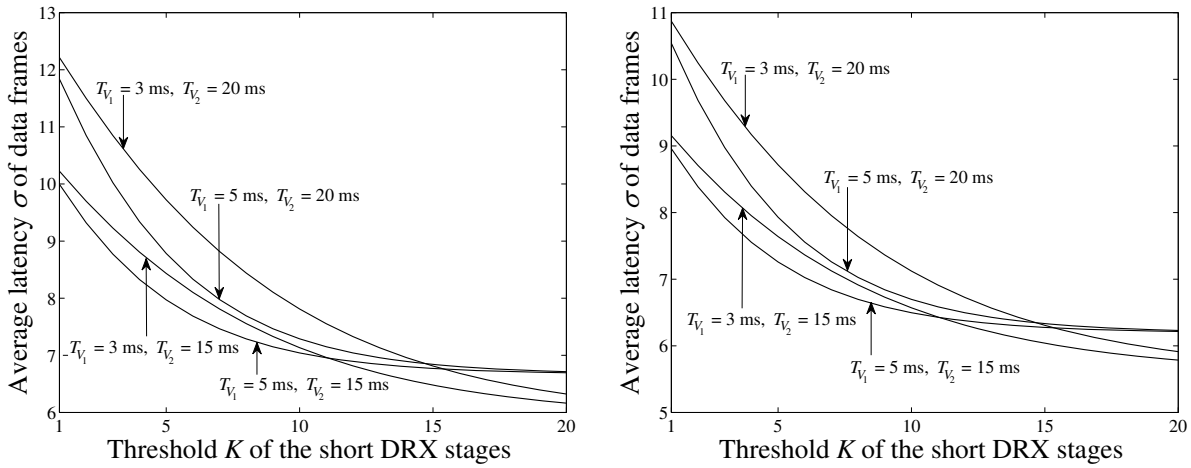

(a) $T = 5$ ms (b) $T = 10$ ms

FIGURE 5. Change trend of the average latency of data frames

From Figures 5(a) and 5(b), we notice that for the same time lengths T_{V_1} of the short DRX stage and T_{V_2} of the long DRX stage, when the threshold K increases, the average latency of data frames σ will decrease. This is because as the threshold K increases, the number of the short DRX stages in a DRX cycle will increase, the data frames will more likely arrive in the short DRX stages, and the system will switch into the working state earlier, so the average latency of data frames will decrease.

In Figures 5(a) and 5(b), we observe that for the same time length T_{V_2} of the long DRX stage, when the threshold K is smaller, the shorter the time length T_{V_1} of the short DRX stage is, and the greater the average latency of data frames σ will be. For example, for the case of $T_{V_2} = 15$ ms and $K < 11$ in Figure 5(a), the average latency of data frames σ with $T_{V_1} = 3$ ms is greater than the average latency of data frames σ with $T_{V_1} = 5$ ms.

Note that a lower threshold K means a fewer short DRX stages in a DRX cycle. In this case, if the time length T_{V_1} of the short DRX stage is shorter, the system will more likely enter the long DRX stage from the short DRX stage. If there is a data frame arrival in a long DRX stage, the system will have to wait for the end of that long DRX stage and then initiate the wake-up procedure, so the average latency will be greater.

However, when the threshold K is big enough, for example $K \geq 11$, the shorter the time length T_{V_1} of the short DRX stage is, the lower the average latency of data frames σ will be. Note that when the threshold K is higher, the number of the short DRX stages will be larger, and the data frames will more likely arrive in the short DRX stages. If the time length T_{V_1} of the short DRX stage is shorter, the system will respond more quickly when there is a data frame arrival in the short DRX stage, so the average latency of data frames will be lower.

Additionally, Figures 5(a) and 5(b) illustrate that for the same threshold K, the same time lengths T of the sleep-delay timer and T_{V_1} of the short DRX stage, a shorter time length T_{V_2} of the long DRX stage will lead to a lower average latency of data frames σ. This is because if a data frame arrives during the long DRX stage, the system will have to wait a long time for the end of that long DRX stage, and then initiate the wake-up procedure and enter into the working state. Therefore, the shorter the long DRX stage is, the lower the average latency of data frames will be.

Moreover, by comparing Figure 5(a) with Figure 5(b), we conclude that for the same threshold K, and the same time lengths T_{V_1} of the short DRX stage and T_{V_2} of the long DRX stage, the average latency of data frames σ with a longer time length T of the sleep-delay timer is lower than that one with a shorter time length T. The reason is that the system will return to the working state at once if there is a data frame arrival in the sleep-delay period. So when the time length T is greater, the average latency of data frames will be lower.

5.2. **System optimizations.** From Figures 3-5, we conclude that there is a trade-off between different performance measures. Aiming to optimize the threshold K of the short DRX stages and the time length T of the sleep-delay timer, we construct a cost function $F(X)$ as follows:

$$F(X) = C_1\beta + \frac{C_2}{\gamma} + C_3\sigma \tag{30}$$

where C_1 and C_3 are the factors of the handover ratio and the average latency of data frames to the system cost, respectively. C_2 is the factor of the energy saving ratio in relation to the system reward. C_1, C_2 and C_3 are all system parameters and they are variable in different numerical examples as required in practice.

We can obtain the cost function $F(K)$ when we set X of Equation (30) to K versus the threshold K of the short DRX stages by fixing the time length T of the sleep-delay timer, or the cost function $F(T)$ when we set X of Equation (30) to T versus the time length T of the sleep-delay timer by fixing the threshold K of the short DRX stages, where β, γ and σ are given by Equation (27), Equation (28) and Equation (29), respectively. β, γ and σ are all the functions of T and K.

In the following numerical results, we let $C_1 = 1.3$, $C_2 = 1.0$ and $C_3 = 1.9$ as an example by referencing [1]. The change trend of the cost function $F(K)$ versus the threshold K of the short DRX stages with different time lengths T_{V_1} of the short DRX stage and T_{V_2} of the long DRX stage is shown in Figure 6.

Figure 6 illustrates that as the threshold K increases, the cost function $F(K)$ will experience two stages. Note that as the threshold K increases, the number of the short DRX stages in a DRX cycle will be greater. During the first stage, the cost function $F(K)$

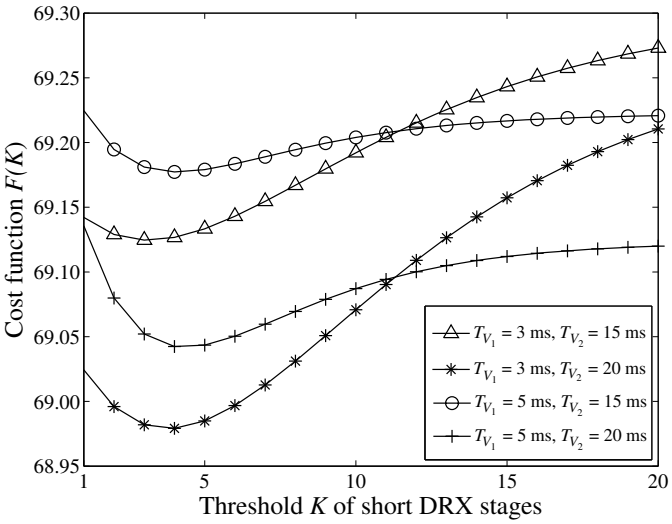

FIGURE 6. Cost function $F(K)$ versus the threshold K of short DRX stages ($T = 10$ ms)

will decrease as the threshold K increases. If there is a data frame arrival in the short DRX stage, the system will enter into a working state quickly and respond rapidly, and the average latency of data frames will be lower. On the other hand, if no data frames arrive in the short DRX stages, the system will enter the long DRX stage easily after a number of the short DRX stages reach the threshold K. Consequently, more energy will be saved. In this case, the cost function $F(K)$ will decrease.

During the next stage, the cost function $F(K)$ will increase as the threshold K continues increasing. The data frames will more likely arrive in the short DRX stages and the system will switch into the working state quickly, so the handover ratio will inevitably increase. If there are no data frame arrivals during the short DRX stages, the system will not enter the long DRX stages easily, not until the number of the short DRX stages reaches K. This means there will be less energy conservation. In this case, the cost function $F(K)$ will be greater. This shows conclusively that when the threshold is set to an optimal value, there is a minimum cost for all the time lengths of the short DRX stage and the long DRX stage.

We set the time length T of the sleep-delay timer as $T = 10$ ms. With different time lengths T_{V_1} of the short DRX stage and T_{V_2} of the long DRX stage, the optimal thresholds K^* and the minimum costs $F(K^*)$ are presented in Table 1.

TABLE 1. Optimal threshold K^* of the short DRX stages

T_{V_1}	T_{V_2}	K^*	$F(K^*)$
3	15	3	69.1246
3	20	4	68.9792
5	15	4	69.1773
5	20	4	69.0424

The change trend of the cost function $F(T)$ versus the time lengths T of the sleep-delay timer with different time lengths T_{V_1} of the short DRX stage and T_{V_2} of the long DRX stage is shown in Figure 7.

From Figure 7, we find that as the time length T of the sleep-delay timer increases, the cost function $F(T)$ will experience two stages. During the first stage, the cost function $F(T)$ will decrease as the time length T increases. The reason is that when the time

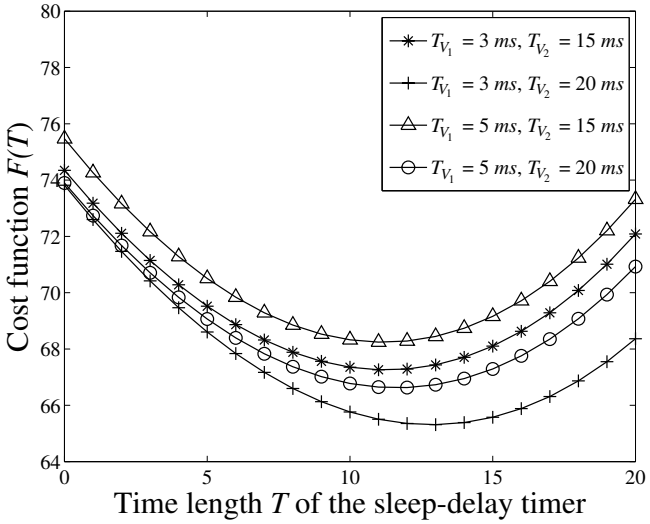

FIGURE 7. Cost function $F(T)$ versus the time length T of the sleep-delay timer ($K = 5$)

length T of the sleep-delay timer is shorter, and as the time length T increases, the more likely it is that a data frame will arrive within the time length of the sleep-delay timer. The system will more likely enter the working state at once, and the average latency of data frames will be lower. Therefore, the cost function $F(T)$ will decrease.

During the next stage, the cost function $F(T)$ will increase as the time length T becomes longer and longer. This is because when the time length T of the sleep-delay timer is long, if there is no data frame arrival within T, the system will have to wait for the sleep-delay timer to expire before it can enter the DRX stage, thus reducing the level of energy conservation. Therefore, the cost function $F(T)$ will be greater. This leads to the conclusion that when the time length of the sleep-delay timer is set to an optimal value, there will be a minimum cost for all the time lengths of the short DRX stage and the long DRX stage.

Note that when the time length of the sleep-delay timer is 0 ms, the enhanced energy saving strategy proposed in this paper will be downgraded to a conventional energy saving strategy for an Active DRX in LTE. From the change trend shown in Figure 7, we see that the cost of the conventional energy saving strategy is higher than that of the enhanced energy saving strategy when the time length of the sleep-delay timer T is set reasonably.

When the threshold K of the short DRX stages is set as $K = 5$, with different time lengths T_{V_1} of the short DRX stage and T_{V_2} of the long DRX stage, the optimal time lengths T^* of the sleep-delay timer and the minimum costs $F(T^*)$ are shown in Table 2.

TABLE 2. Optimal time length T^* of the sleep-delay timer

T_{V_1}	T_{V_2}	T^*	$F(T^*)$
3	15	12	67.2612
3	20	13	65.3125
5	15	12	68.2427
5	20	12	66.6293

6. **Conclusions.** In this paper, we have proposed an enhanced energy saving strategy for an Active DRX in LTE by introducing a sleep-delay mechanism and considering a waking-up procedure. Accordingly, we built a discrete-time multiple vacation queueing

model with a vacation-delay period and a set-up period. Moreover, we have analyzed the system model in the steady state by using an embedded Markov chain and calculated the formulas for the performance measures, including the handover ratio, the energy saving ratio, and the average latency of data frames. Using numerical experiments, we have demonstrated the impact of the different thresholds of the short DRX stages, the different time lengths of the sleep-delay timer, the short DRX stage, and the long DRX stage on the system performance. We have also investigated the trade-off between different performance measures. Finally, we have optimized the threshold of the short DRX stages and the time length of the sleep-delay timer while minimizing the cost functions. This paper has potential applications in the improvement of energy saving strategies for wireless communication networks.

Acknowledgment. This work is supported by Hebei Province Science Foundation (No. F2012203093), China and was supported in part by MEXT, Japan. The authors also gratefully acknowledge the helpful comments and suggestions of the reviewers, which have improved the presentation.

REFERENCES

[1] S. Jin and W. Yue, Performance analysis for power saving class type of IEEE 802.16 in WiMAX, *Computer Networks*, vol.55, no.16, pp.3734-3743, 2011.

[2] J. Wigard, T. Kolding, L. Dalsgaard and C. Coletti, On the user performance of LTE UE power saving schemes with discontinuous reception in LTE, *IEEE International Conference on Communications Workshops*, pp.1-5, 2009.

[3] S. Abeta, Toward LTE commercial launch and future plan for LTE enhancements (LTE-advanced), *Proc. of IEEE International Conference on Communication Systems*, pp.146-150, 2010.

[4] Y. Mihor, K. Kasser and B. Tsankov, Analysis and performance evaluation of the DRX mechanism for power saving in LTE, *Proc. of IEEE the 26th Convention of Electrical and Electronics Engineering*, pp.520-524, 2010.

[5] K. Ting, H. Wang, C. Tseng et al., Energy-efficient DRX scheduling for QoS traffic in LTE network, *Proc. of IEEE the 9th International Symposium on Parallel and Distributed Processing with Applications*, pp.213-218, 2011.

[6] J. Luo, C. Liu and Z. Shao, The analysis of next generation mobile network discontinuous reception mechanism on mobile Internet business performance, *Telecommunications Science*, vol.27, no.7, pp.29-34, 2011 (in Chinese).

[7] C. Bontu and E. Illidgee, DRX mechanism for power saving in LTE, *IEEE Communications Magazine*, vol.47, no.6, pp.48-55, 2009.

[8] F. Yin, An application aware discontinuous reception mechanism in LTE-advanced with carrier aggregation consideration, *Annales Des Telecommunications-Annals of Telecommunications*, vol.67, nos.3-4, pp.147-159, 2012.

[9] R. Li, C. Zhang and X. Ning, Improved algorithm of DRX mechanism in long term evolution system, *Journal of Computer Applications*, vol.30, no.12, pp.3187-3190, 2010 (in Chinese).

[10] 3GPP TS 36.321, Technical specification group radio access network, evolved universal terrestrial radio access (E-UTRA), *Medium Access Control (MAC) Protocol Specification*, 2008.

[11] S. Jin, W. Yue and Q. Sun, Performance analysis of the sleep/wakeup protocol in a wireless sensor network, *International Journal of Innovative Computing, Information and Control*, vol.8, no.5(B), pp.3833-3844, 2012.

[12] D. Nga and H. Lim, Power-saving mechanism with delay bound for mobile WiMAX systems, *IET Communications*, vol.5, no.13, pp.1854-1859, 2011.